The Equatorial Ridges of Pan and Atlas: Terminal Accretionary Ornaments?

Sébastien Charnoz, *et al.*

Science **318**, 1622 (2007);
DOI: 10.1126/science.1148631

the Cassie state with water and various organic liquids. The presence of re-entrant curvature, though, is not a sufficient condition for developing highly nonwetting surfaces; the Cassie state may be inaccessible in practice if the applied pressure (or energy barrier) required to transition from the Cassie to the Wenzel state is small. However, by independently controlling both the chemical and topographic nature of surfaces (as embodied in two dimensionless design parameters, D^* and H^*), we have shown that it is possible to design extremely robust nonwetting surfaces.

References and Notes

1. W. Barthlott, C. Neinhuis, *Planta* **202**, 1 (1997).
2. S. Herminghaus, *Europhys. Lett.* **52**, 165 (2000).
3. X. Gao, L. Jiang, *Nature* **432**, 36 (2004).
4. A. R. Parker, C. R. Lawrence, *Nature* **414**, 33 (2001).
5. K. Autumn *et al*., *Nature* **405**, 681 (2000).
6. J. Genzer, K. Efimenko, *Biofouling* **22**, 339 (2006).
7. R. N. Wenzel, *Ind. Eng. Chem.* **28**, 988 (1936).
8. A. B. D. Cassie, S. Baxter, *Trans. Faraday Soc.* **40**, 546 (1944).
9. M. Callies, D. Quere, *Soft Mat.* **1**, 55 (2005).
10. A. Marmur, *Langmuir* **19**, 8343 (2003).
11. M. Nosonovsky, *Langmuir* **23**, 3157 (2007).
12. A. Nakajima, K. Hashimoto, T. Watanabe, *Monatsh. Chem.* **132**, 31 (2001).
13. D. Quere, *Rep. Prog. Phys.* **68**, 2495 (2005).
14. S. R. Coulson, I. S. Woodward, J. P. S. Badyal, S. A. Brewer, C. Willis, *Chem. Mater.* **12**, 2031 (2000).
15. K. Tsujii, T. Yamamoto, T. Onda, S. Shibuichi, *Angew. Chem. Int. Ed. Engl.* **36**, 1011 (1997).
16. S. Shibuichi, T. Yamamoto, T. Onda, K. Tsujii, *J. Colloid Interface Sci.* **208**, 287 (1998).
17. W. Chen *et al*., *Langmuir* **15**, 3395 (1999).
18. M. Zhu, W. Zuo, H. Yu, W. Yang, Y. Chen, *J. Mater. Sci.* **41**, 3793 (2006).
19. See supporting material on *Science* Online.
20. L. Gao, T. J. McCarthy, *Langmuir* **23**, 3762 (2007).
21. Recent work by McCarthy and colleagues (*20*) points out that these models are applicable only at the solid-liquid-vapor three-phase contact line (drop perimeter) and that the interfacial area within the drop perimeter does not affect either the apparent contact angle or the hysteresis; thus, these models can be easily applied only to surfaces with a homogeneous texture, as considered here.
22. T. Young, *Philos. Trans. R. Soc. London* **95**, 65 (1805).
23. N. A. Patankar, *Langmuir* **19**, 1249 (2003).
24. B. He, N. A. Patankar, J. Lee, *Langmuir* **19**, 4999 (2003).
25. T. N. Krupenkin *et al*., *Langmuir* **23**, 9128 (2007).
26. L. Barbieri, E. Wagner, P. Hoffmann, *Langmuir* **23**, 1723 (2007).
27. A. Lafuma, D. Quere, *Nat. Mater.* **2**, 457 (2003).
28. W. A. Zisman, in *Contact Angle, Wettability and Adhesion*, F. M. Fowkes, Ed. (American Chemical Society, Washington, DC, 1964), pp. 1–51.
29. Y.-T. Cheng, D. E. Rodak, *Appl. Phys. Lett.* **86**, 144101 (2005).
30. D. E. Suk *et al*., *Macromolecules* **35**, 3017 (2002).
31. D. H. K. Pan, W. M. Prest Jr., *J. Appl. Phys.* **58**, 2861 (1985).
32. D. H. Reneker, A. L. Yarin, H. Fong, S. Koombhongse, *J. Appl. Phys.* **87**, 4531 (2000).
33. M. Ma, Y. Mao, M. Gupta, K. K. Gleason, G. C. Rutledge, *Macromolecules* **38**, 9742 (2005).
34. M. Ma *et al*., *Adv. Mater.* **19**, 255 (2007).
35. H. Fong, I. Chun, D. H. Reneker, *Polym.* **40**, 4585 (1999).
36. L. Feng *et al*., *Angew. Chem.* **116**, 2046 (2004).
37. These surfaces are referred to as micro-hoodoos because their geometry and process of creation are reminiscent of geological features called hoodoos, which are created by soil erosion. Hoodoos are composed of a soft sedimentary rock topped by a piece of harder, less easily eroded stone.
38. Because $2D << (\gamma_{lv}/\rho g)^{0.5}$ (capillary length; ρ is the density of liquid), the effect of gravity is negligible and we approximate the liquid-air interface to be a horizontal plane.
39. Nosonovsky (*11*) recently derived another important criterion for the creation of a local minimum in free energy, and thus for the creation of a stable heterogeneous interface: $dA_{sl}d\theta < 0$, where dA_{sl} is the change in solid-liquid contact area with the advancing or receding of the liquid, and $d\theta$ is the change in local contact angle. This criterion also emphasizes the importance of re-entrant surfaces.
40. L. Cao, H. H. Hu, D. Gao, *Langmuir* **23**, 4310 (2007).
41. As the surface is pushed toward the water droplet, the droplet moves, and hence the normal force is not transferred perfectly.
42. The difference in contact angle values from the Cassie prediction is related to contact line pinning.

43. Supported by Air Force Research Laboratory contract FA9300-06M-T015 and Air Force Office of Scientific Research contracts FA9550-07-1-0272 and LRIR-92PL0COR, with additional student support provided by the NSF Nanoscale Interdisciplinary Research Team on Nanoscale Wetting (DMR-0303916). We thank the Institute for Soldier Nanotechnologies at MIT for the use of facilities.

Supporting Online Material

www.sciencemag.org/cgi/content/full/318/5856/1618/DC1
Materials and Methods
SOM Text
Figs. S1 to S10
Tables S1 to S3
References
Movies S1 to S4

25 July 2007; accepted 22 October 2007
10.1126/science.1148326

The Equatorial Ridges of Pan and Atlas: Terminal Accretionary Ornaments?

Sébastien Charnoz,[1]* André Brahic,[1] Peter C. Thomas,[2] Carolyn C. Porco[3]

In the outer regions of Saturn's main rings, strong tidal forces balance gravitational accretion processes. Thus, unusual phenomena may be expected there. The Cassini spacecraft has recently revealed the strange "flying saucer" shape of two small satellites, Pan and Atlas, located in this region, showing prominent equatorial ridges. The accretion of ring particles onto the equatorial surfaces of already-formed bodies embedded in the rings may explain the formation of the ridges. This ridge formation process is in good agreement with detailed Cassini images showing differences between rough polar and smooth equatorial terrains. We propose that Pan and Atlas ridges are kilometers-thick "ring-particle piles" formed after the satellites themselves and after the flattening of the rings but before the complete depletion of ring material from their surroundings.

In images sent by the Voyager spacecraft in the early 1980s, two small satellites were discovered orbiting inside Saturn's rings (*1*, *2*), where Roche (*3*) had shown that strong tidal forces prevent the formation of any big satellite. Pan is located in the A ring's Encke Gap at 133,600 km from Saturn's center, and Atlas orbits at 137,700 km from Saturn's center, just outside the A ring. The Cassini spacecraft has recently resolved them both. Their shapes (Fig. 1) are close to oblate ellipsoids, with equatorial radii of 16.5 and ~19.5 km, and polar radii of ~10.5 km and 9 km for Pan and Atlas, respectively. These dimensions (*4*) are close to the moons' Hill radii (corresponding to the satellites' gravitational cross sections). More unexpectedly, both have a prominent equatorial ridge. These ridges are roughly symmetric about the bodies' equators and give them the appearance of a "flying saucer." Assuming that Pan and Atlas are rotating synchronously around Saturn (like the Moon around the Earth), consistent with Cassini images taken at several different times (*5*), Pan's ridge extends from –15° to +15° latitude (±~5°) and apparently entirely encircles the satellite. Atlas' ridge extends from –30° to +30° latitude (±10°) on the trailing side, whereas on the leading side the ridge is much less prominent, with a modest depression on the leading side near the equator (*4*) (Fig. 1C).

Recent work (*6*) has shown that a fast rotation may explain the diamond shape of the near-earth asteroid 1999 KW4 because of the balance of the centrifugal and gravity forces at the asteroid's equator. This mechanism seems, however, inadequate to explain the shapes of Pan and Atlas: Their rotation periods T (~14 hours) are much too long for centrifugal forces to balance surface gravity (which requires $T \sim 5$ hours). In addition, Saturn's tidal stress would elongate the moons in the radial direction (*3*, *7*) rather than create an equatorial ridge. Therefore, neither centrifugal nor tidal forces seem adequate to explain these ridges.

A number of circumstances led us to investigate a different scenario for the creation of the ridges: (i) Contrary to other resolved satellites, Pan and Atlas are embedded in Saturn's rings. (ii) The ridges are equatorial and precisely in the same plane as Saturn's rings. (iii) The vertical motion of Atlas (and perhaps Pan) through the rings is approximately equal to the

[1]Laboratoire AIM, Commissariat à l'Énergie Atomique (CEA)/Université Paris 7/CNRS, 91191 Gif-sur-Yvette Cedex, France. [2]Center for Radiophysics and Space Research, Cornell University, Ithaca, NY 14853, USA. [3]Cassini Imaging Central Laboratory for Operations, Space Science Institute, Boulder, CO 80301, USA.

*To whom correspondence should be addressed: charnoz@cea.fr

vertical extent of the ridges (*8*). (iv) The total volume of the ridges is ~10 to 25% of the bodies' volume (*4*). Therefore, we have explored the possibility that the ridges are made of ring particles accreted lately onto the surface of a preexisting moonlet embedded in the rings and initially free of any equatorial ridge. Then, a ridge would be simply an "equatorial ornament" accumulated onto the body's surface as a later stage in the formation process.

For a satellite with an orbital inclination i, semimajor axis a_s, and radius r, the latitudinal extension of the intersection of the ring plane with the body's surface is $L = \sin^{-1}(ia_s/r)$, assuming a vertical thickness h of the rings, much smaller than the satellite radius r, consistent with observations and models (*9*, *10*). Ring particles may collide between latitudes –L and +L. Using the average radii of Pan and Atlas (*4*) and their last published inclinations (0.001° and 0.003°, respectively) (*8*), we get, respectively, $L = \pm 12°$ and $L = \pm 28°$, in good agreement with observations. Atlas's inclination likely results from Prometheus's gravitational perturbations (*5*, *8*).

To simulate the fall of ring particles onto the surface of Pan and Atlas, a dynamical code (*11*) is used in which the orbits of Pan, Atlas, and 10^4 massless test particles are integrated, accounting for Saturn's J2 and J4 gravitational moments (*12*). The Pan and Atlas precursors have shapes similar to their actual ones but with equatorial radii smaller by ~10% to account for the initial absence of the ridges. Synchronous rotation is assumed. The test particles are initially gathered into a thin ring with vertical thickness $h = 250$ m, so that $h/r << 1$. Locations of impacts at the surface of the satellites are detected and located in the satellite's east longitude and latitude system (Fig. 2). Because of computer limitations, collisions between ring particles were ignored, but this approximation does not alter the latitudinal impact distribution as long as the ring system remains thin during the ridge accretion process, which is indeed the case throughout the simulation (SOM Text). Collisions would, however, modify the final longitudinal distribution, especially when the ridge accumulates on the satellite surface, so our simulation must be considered as a first-order model of the initial steps of ridge accretion.

The simulations show that impacts are concentrated near the equator (Fig. 2), with latitudinal ranges ±10° for Pan and ±30° for Atlas, in agreement with the observations (Fig. 1, A and B). Impacts on Atlas's surface near its leading (270° longitude) and trailing (90° longitude) points show a wider spread in latitude: This is a consequence of Atlas's much flatter shape compared with Pan. Unexpectedly, ring-particles' distribution of impacts appears to be strongly segregated: Particles with initial semimajor axes inward of their respective satellite ("inner particles") and those outward of the satellite ("outer particles") impact on different hemispheres (crosses and open diamonds in Fig. 2). For Pan, inner particles impact on the hemisphere facing Saturn and outer particles impact on the hemisphere opposite Saturn. For Atlas, the distributions are shifted by 90° compared with Pan: Inner particles collide on the leading hemisphere, and outer particles collide on the trailing hemisphere.

These different distributions are likely the consequences of the satellites' different eccentricities (3.5×10^{-5} and 1.2×10^{-3} for Pan and Atlas, respectively) (*8*). An orbital eccentricity e implies a radial excursion $\Delta r = \pm a_s e$. For Pan, $\Delta r = \pm 5$ km, which is much smaller than Pan's Hill radius of 19.5 km. Conversely, the Atlas radial excursion is ±165 km, much larger that its Hill radius of 23 km. Thus, different accretion processes must be considered for the two satellites: a low-velocity scenario for Pan and a high-velocity one for Atlas.

As a result of Pan's (almost) circular orbit, ring particles reach Pan's surface with low relative velocities. Therefore, classical celestial mechanics (*7*) tells us that particles must pass through Pan's L1 or L2 Lagrange points (the gates for entering the moon's Hill sphere). Inner particles flow through the L1 point (facing the sub-Saturn point), and outer particles flow through the L2 point (facing the anti-Saturn point). Once a particle penetrates Pan's Hill sphere, its trajectory has no space in which to randomize because the satellite fills almost all

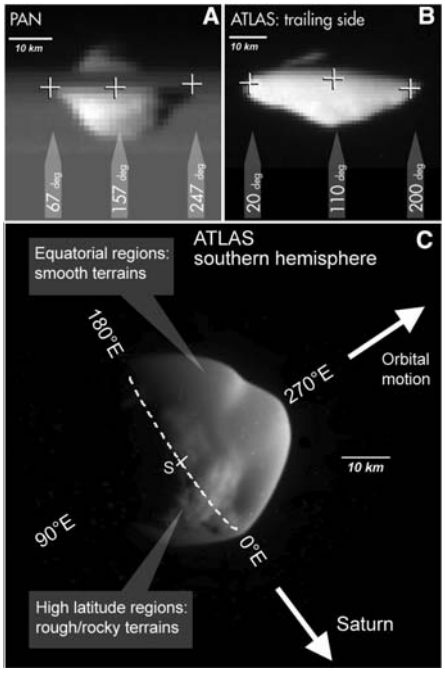

Fig. 1. Cassini narrow-angle camera (NAC) images in clear filter. (**A**) Pan in the Encke gap (1.3 km/pixel). Crosses are located on the body's equator with their corresponding longitude. (**B**) Atlas's trailing side with resolution 1.05 km/pixel. (**C**) High-resolution image of Atlas (320 m/pixel). The South Pole is designated by an "S"; the dashed line is the frontier between the leading and trailing sides. An east-longitude system is used, in which longitudes 0°, 90°, 180°, and 270° correspond to the sub-Saturn points, trailing points, anti-Saturn points, and leading points, respectively. White spots are cosmic rays.

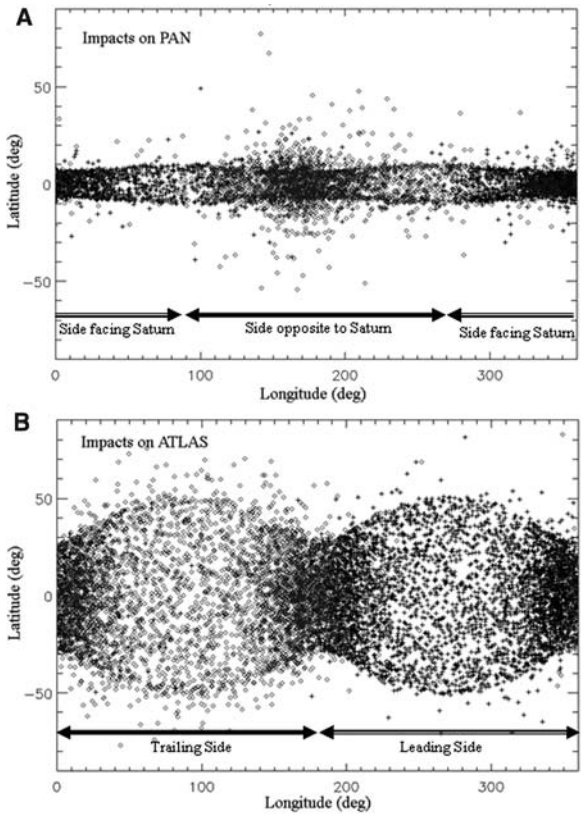

Fig. 2. Impact locations of particles at the surface of Pan (**A**) and Atlas (**B**). Open diamonds, particles initially exterior to the satellite's orbit; black crosses, particles initially interior to the satellite's orbit.

the space inside the Hill sphere (*4*). As a result, particle impacts Pan's surface almost immediately after passing the Lagrange point. This explains the segregation between the two hemispheres (Fig. 3), as well as the observation that the equatorial ridge encircles both hemispheres: Pan accretes material coming from both sides of its orbit.

Atlas, on the other hand, has a large eccentricity. Thus, in the local rotating frame, Atlas makes a clockwise elliptical epicycle with a 2:1 ratio (*7*), with its radial excursion Δr extending much beyond its Hill sphere. In the inner portion of the epicycle in which $r_s < a_s$, (where r_s is the instantaneous satellite's distance to Saturn), Atlas orbits at a higher velocity than the local Keplerian velocity, so inner particles are accreted onto Atlas's leading hemisphere. Conversely, on the outer portion of its epicycle ($r_s > a_s$), Atlas orbits at a lower velocity than the local Keplerian velocity, so outer particles are accreted on the trailing hemisphere only (Fig. 3B). This peculiar local dynamic may explain the differences observed between the trailing and leading sides of Atlas: It may have accreted material coming preferentially from outside its orbit rather than from inside, resulting in a less prominent bulge on the leading hemisphere (*4*).

Therefore, Pan and Atlas may have formed in two steps: an early stage in which a primordial body formed with roughly the current ellipsoidal shape but without an equatorial ridge, and a secondary stage in which the equatorial ridge is accreted from ring material. Consequently, differences between polar and equatorial terrains may be expected. This prediction has been confirmed by a June 13, 2007, high-resolution Cassini image (*4*) of Atlas's southern hemisphere (Fig. 1C). It shows two types of terrains: high-latitude regions (>40° south latitude) with a rough surface texture and equatorial regions (<30° south latitude) with a very smooth surface and no structure down to pixel resolution. A smooth surface is compatible with an accumulation of ring particles that are known to range from millimeters to meters, well below the camera resolution (*13*). Simulations also show that impacts on Pan and Atlas occur preferentially at sub- and anti-Saturn points (fig. S1), implying more elongated ridges in their radial direction. This seems marginally inconsistent with observations (*4*) (Fig. 1C). Our results apply to the early phase of ridge formation and, in reality, later evolutionary processes such as material redistribution, satellite reorientation, and the escape of material through the L1 and L2 Lagrange points will alter the final shape.

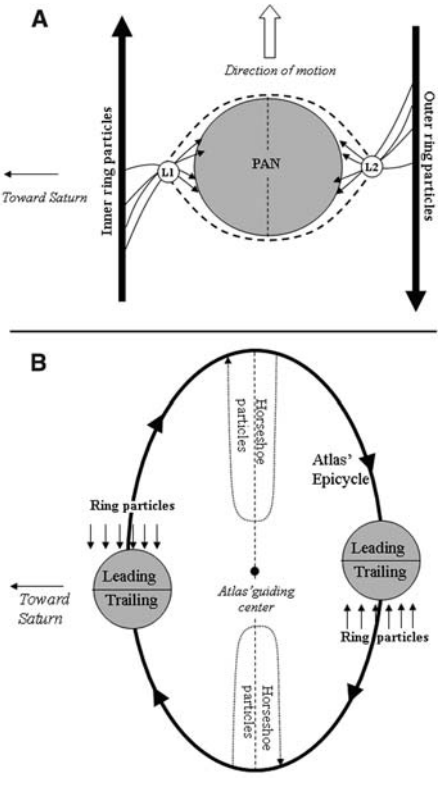

Fig. 3. (**A**) Sketch of the accretion process for Pan. Pan is on a quasicircular orbit. Arrows indicate trajectories of particles entering the Hill sphere of Pan. L1 and L2 stand for the two Lagrange points. (**B**) Sketch of the accretion process for Atlas. Relative sizes of Atlas and its epicycle are not to scale.

To have ridges confined to the equator, the incoming material must remain on very low inclination orbits ($<2 \times 10^{-3}$°) despite the satellite's gravitational stirring (*14*). Therefore, either (i) the ridge is accreted rapidly, as simulated here, or (ii) a dissipative environment is present to damp incoming particles' inclinations. A recent work (*4*) suggests that Pan, and maybe Atlas, opened a gap before completing accretion. So, ridge accretion may have happened after the start of the gap opening but before the complete emptying of the satellites' surroundings. This suggests that a transition phase may have existed: while a gap was already opened, the satellite could be fed by an accretion disk flowing from the gap's edges, like for giant-planet formation in the protoplanetary disk. If needed, dissipative collisions would also lower Pan's inclination. Conversely, Atlas's inclination, being gravitationally forced by Prometheus (*8*), remains nonzero

Voyager (*2*) and Cassini images (*15*) show the presence of tenuous material in the Pan and Atlas regions, and we examined whether this material could be accumulated onto the ridges. Our simulations show (fig. S2), on the one hand, that the material in the ringlet close to Pan is prevented from reaching Pan's surface because it is on horseshoe orbits and Pan is on a nearly circular orbit. On the other hand, because of Atlas's substantial inclination, the surrounding material is vertically stirred rapidly (fig. S3) and is prevented from accumulating specifically at Atlas's equator. So, a recent accretion of ridges from the material in the Encke gap or in the Atlas region seems unlikely, although some contribution cannot be completely discarded.

These results, together with other evidence collected by Cassini (*4*), suggest a relative chronology for the formation of Saturn's rings and the ridges of Pan and Atlas. The process by which Saturn's rings formed is still open to discussion (*16*, *17*). However, if a catastrophic breakup of a larger body happened, the cores of Pan and Atlas would have been among the largest fragments, orbiting initially on an inclined and eccentric orbit. Then, a two-step process may have occurred: Before the flattening of the rings, these shards accreted a shell of debris coming from the surrounding disk, giving them their low density and overall Roche lobe size (*4*). Once the debris disk flattened into a thin ring system due to dissipative collisions, ring material accreted at the satellites' equator through an accretion disk as outlined herein, forming today's ridges as observed by Cassini.

These ridges may also be of interest for planetary formation: They could be considered as "fossilized" accretion disks that once may have surrounded Pan and Atlas, like small-scale versions of the planetary subnebulas that once surrounded the giant planets. Such fossilized disks may result from two extreme characteristics of small satellites in planetary rings: (i) In rings, the ratio of the disk's thickness to the satellite's size is much smaller than unity, so that material flows toward the satellite's equator. (ii) In rings, it has been found that these satellites completely fill their Hill spheres (*4*) so that the trapped material is squeezed at the body's surface and accumulates immediately, forming today's equatorial ridges.

References and Notes

1. M. R. Showalter, *Nature* **351**, 709 (1991).
2. B. A. Smith *et al.*, *Science* **212**, 163 (1981).
3. E. Roche, *Mémoires de la Section des Sciences. Académie des Sciences et Lettres de Montpellier* **1**, 243 (1849).
4. C. C. Porco, P. C. Thomas, J. W. Weiss, D. C. Richardson, *Science* **318**, 1602 (2007).
5. C. C. Porco *et al.*, *Bull. Am. Astr. Soc.* **37**, 768 (2005).
6. S. J. Ostro *et al.*, *Science* **314**, 1276 (2006).
7. H. Poincaré, *Leçons de Mécanique Céleste* (Gauthier-Villars, Paris, 1905).
8. J. N. Spitale, R. A. Jacobson, C. C. Porco, W. M. Owen, *Astron. J.* **132**, 692 (2006).
9. A. Brahic, B. Sicardy, *Nature* **289**, 447 (1981).
10. J. A. Cowell, L. W. Esposito, M. Sremčević, *GeoRL* **33**, L07201 (2006).
11. S. Charnoz, P. Thébault, A. Brahic, *Astron. Astrophys.* **373**, 683 (2001).
12. J. K. Campbell, J. D. Anderson, *Astron. J.* **97**, 1485 (1989).
13. H. A. Zebker, E. A. Marouf, G. L. Tyler, *Icarus* **64**, 531 (1985).
14. R. Karjalainen, H. Salo, *Icarus* **172**, 328 (2004).
15. C. C. Porco *et al.*, *Science* **307**, 1226 (2005).
16. A. Harris, in *Planetary Rings*, R. Greenberg, A. Brahic, Eds. (Univ. Arizona Press, 1984), pp. 641–659.
17. M. S. Tiscareno *et al.*, *Nature* **440**, 648 (2006).
18. C.C.P. and P.C.T. acknowledge the support of NASA/JPL and the Cassini Project. We thank J. Colwell and H. Throop for careful reading, F. Durillon for graphics, and three anonymous referees.

Supporting Online Material

www.sciencemag.org/cgi/content/full/318/5856/1622/DC1
SOM Text
Figs. S1 to S3

1 August 2007; accepted 4 October 2007
10.1126/science.1148631